FEBS Letters

An additional cysteine in a typical 2-Cys peroxiredoxin of *Pseudomonas* promotes functional switching between peroxidase and molecular chaperone

Byung Chull An [a], Seung Sik Lee [a], Hyun Suk Jung [b], Jin Young Kim [c], Yuno Lee [d], Keun Woo Lee [d], Sang Yeol Lee [d], Bhumi Nath Tripathi [a], Byung Yeoup Chung [a,*]

[a] Advanced Radiation Technology Institute, Korea Atomic Energy Research Institute, 29 Geumgu-gil, Jeongeup 580-185, Republic of Korea
[b] Department of Biochemistry, College of Natural Sciences, Kangwon National University, Chuncheon 200-701, Republic of Korea
[c] Division of Mass Spectrometry Research, Korea Basic Science Institute, 162 Yeongudanjiro, Ochang 363-883, Republic of Korea
[d] Division of Applied Life Science (Brain Korea 21 Program), Gyeongsang National University, 501 Jinju-daero, Jinju 660-701, Republic of Korea

ARTICLE INFO

ABSTRACT

Peroxiredoxins (Prx) have received considerable attention during recent years. This study demonstrates that two typical *Pseudomonas*-derived 2-Cys Prx proteins, PpPrx and PaPrx can alternatively function as a peroxidase and chaperone. The amino acid sequences of these two Prx proteins exhibit 93% homology, but PpPrx possesses an additional cysteine residue, Cys112, instead of the alanine found in PaPrx. PpPrx predominates with a high molecular weight (HMW) complex and chaperone activity, whereas PaPrx has mainly low molecular weight (LMW) structures and peroxidase activity. Mass spectrometry and structural analyses showed the involvement of Cys112 in the formation of an inter-disulfide bond, the instability of LMW structures, the formation of HMW complexes, and increased hydrophobicity leading to functional switching of Prx proteins between peroxidase and chaperone.

© 2015 Federation of European Biochemical Societies. Published by Elsevier B.V. All rights reserved.

1. Introduction

2-Cys peroxiredoxin (typical 2-Cys Prx) is one of the most studied PRX due to its well established metabolic significance in variety of organisms [1–7]. 2-Cys Prx performs several functions, particularly peroxidase, molecular chaperone, thiol oxidase and also modulates cell signaling [8]. In contrast to other peroxidases, 2-Cys Prxs possess an extremely reactive and conserved Cys residue in the active site (peroxidatic Cys; Cys_P) capable to react with hyperoxides and peroxynitrite [9]. Sulfenic acid intermediately formed due to reaction of Cys_P reacts with a second Cys thiol (resolving Cys, Cys_R) of other subunit of the homo-dimer and makes a disulfide bridge. However, this oxidized disulfide form may be reduced (regenerated) back by means of different reductants [10]. But the

sulfenic acid intermediates are susceptible to further oxidation to sulfinic acid leading to switching of its function from peroxidase to molecular chaperone [11].

The capability of dual function (peroxidase and chaperone) of 2-Cys Prx was first identified in 2-Cys Prx 1 (formerly PAG) [12] and subsequently confirmed in other eukaryotes and prokaryotes [1,2,11,13,14]. Environmental cues including oxidative stress and high temperature shifts the quaternary structure of 2-Cys Prx (dimer/decamer) to high molecular weight species with concurrent loss of its peroxidase function and manifestation of molecular chaperone function [2,11,13,14]. However, the key modulators of this functional switch of 2-Cys Prx are not well known. Based on limited information, post-translational modifications/interactions e.g. site-specific phosphorylation, acetylation, covalent/non-covalent interactions, etc. individually or in combination may be predicted as plausible mechanism responsible for the functional switch of 2-Cys Prx. Jang et al. [13] have observed the significant change in the protein structure of human 2-Cys Prx isotype I (hPrxI) from low molecular weight to high molecular weight protein complexes and its dual functions due to phosphorylation. A study on 2-Cys Prx of *Pseudomonas aeruginosa* (PaPrx) suggested the association of peroxidase and chaperone activities of PaPrx

with dissociation of the complexes into low molecular weight species and multimerization of protein complexes, respectively [15]. Hence, the dual functions of 2-Cys Prx are clearly associated with their ability to form distinct protein structures. Saccoccia et al. [7] have attempted to demonstrate the mechanism through which chemical stresses, such as, H_2O_2 and acidic pH render functional switch in a typical 2-Cys Prx of *Schistosoma mansoni* (SmPrxI). Further, Angelucci et al. [16] have proposed the sequence of events starting from the overoxidation of the sulfur atom of Cys_P of SmPrx1, causing destabilization of the α2 helix, followed by unwinding of the first turn of the α2 helix, unfolding of the C-terminal tail and protrusion of the β3-α2 loop toward the nearby dimer leading to quaternary structural changes resulting into the formation of high molecular weight species of SmPrx1 endowed with chaperone activity. The switching between alternative structures and functions of SmPrx1 was also explained by a combination of data produced by X-ray crystallography, transmission electron microscopy (TEM) and site-directed mutagenesis [16]. König et al. [8] have also used several mutants with specific conformational states e.g. peroxidase function (ΔC), hyperoxidized chaperone (C54D) and oxidized inactive protein (C54DC176K) to demonstrate the importance of structural flexibility for switching between peroxidase and chaperone function. Previous studies attempting to explain the mechanism of structural and functional switching of 2-Cys Prx were mainly based on the modification of their reactive cysteines [7,8,16]. But the role of other interacting molecules, proteins or other structural entity of 2-Cys Prx in regulating the functional switching between peroxidase and chaperone is still not known and hence, warrants further research.

Recently, we have identified a novel Prx from *Pseudomonas putida* (PpPrx) having an additional Cys (Cys^{112}) between two conserved Cys residues (with Cys^{51} as the Cys_P and Cys^{171} as the Cys_R) [17]. PpPrx is a kind of typical 2-Cys Prx having highly homologous amino acid sequences with other typical 2-Cys Prx, including PaPrx of *P. aeruginosa* (Fig. S1). Amino acid sequences alignment of PpPrx and PaPrx exhibited 93% homology and 89% identity (Fig. S1), with conserved Cys residues (Cys^{51} and Cys^{171}) that form an intermolecular disulfide bond essential for peroxidase activity. Like other 2-Cys Prx e.g. PaPrx, PpPrx also efficiently displayed the ability of functional switching between peroxidase and molecular chaperone functions [17]. But, being predominated with chaperone function PpPrx exhibited totally contrasting tendency of displaying dual function compared to PaPrx, which is predominated with peroxidase function. This contrasting tendency of PpPrx seems to be associated with the presence of an additional Cys (Cys^{112}) that triggers the conversion of low molecular weight (LMW) form of PpPrx to high molecular weight (HMW) with increased chaperone activity. Based on these facts, the present study is aimed to characterize the importance of the presence of an additional Cys in regulating conformational and functional changes in PpPrx. In contrast to previous studies [7,8,16], we demonstrate the significance of an additional Cys located between two conserved reactive Cys residues of 2-Cys Prx in regulating the structural and functional switching in 2-Cys Prxs of *Pseudomonas* species.

2. Material and methods

2.1. Bacterial strains and materials

The bacterial strains (*P. putida* KT2440, *P. aeruginosa* PAO1, and *Escherichia coli*) used in the present study were cultivated aerobically in LB medium (0.5% sodium chloride, 0.5% yeast extract, and 1% tryptone; DB, Franklin Lakes, NJ, USA) at 30 °C. Two wild types (*WT-PpPrx* and *WT-PaPrx*) and mutant Prxs (*C112S-PpPrx*, *C112A-PpPrx*, and *A112C-PaPrx*) were cloned and expressed in

E. coli KRX cells (Promega, Madison, USA) as described in our previous studies [15,17,18]. The His₆-tagged Prx proteins were isolated by metal-chelate affinity chromatography system using nickel–nitrilotriacetate-agarose (Ni–NTA) (Peptron, Daejeon, Korea). It was further eluted by thrombin in cutting buffer (20 mM Tris–HCl, pH 8.4, 150 mM NaCl) at 4 °C for overnight to remove His-tag to remove the chances of metal interference with purified protein. Purified Prx proteins were dialyzed into 50 mM HEPES (pH 8.0) for biochemical analysis. The concentration of the protein was estimated by Bradford method [19] using bovine serum albumin (BSA) as the standard.

2.2. Size exclusion chromatography (SEC)

SEC was carried out by fast protein liquid chromatography (ÄKTAFPLC; Amersham Biosciences, Piscataway, NJ, USA) using a Superdex 200 10/300 GL column equilibrated at a flow rate of 0.5 mL min⁻¹ at 4 °C with 50 mM HEPES (pH 8.0) buffer containing 100 mM NaCl. Protein peaks obtained at A_{280} were isolated and concentrated using a Centricon YM-30 (Millipore, Massachusetts, USA).

2.3. Peroxidase activity assay

The thioredoxin (Trx)-dependent peroxidase activity of purified Prxs was determined by method as described previously with slight modifications [11,20–22]. Total protein or fractions (F-1 and F-2) separated by SEC were incubated in 50 mM HEPES (pH 8.0) containing 200 μM nicotinamide adenine dinucleotide phosphate (NADPH), 3.0 μM yeast Trx, and 1.5 μM yeast thioredoxin reductase (TR). The reaction mixture was incubated at 30 °C for 5 min and thereafter variable volume of H_2O_2 was added from the stock solution of 0.5 mM so as to obtain desired final concentrations in the solution. NADPH oxidation was monitored by measuring the decrease in absorbance at 340 nm for 6 min using spectrophotometer (Evolution 300 UV–VIS spectrophotometer; Thermoscientific, Worcester, MA, USA).

2.4. Molecular chaperone activity assay

The molecular chaperone activity was assessed by determining the prevention of thermal aggregation of heat-sensitive malate dehydrogenase (MDH) by recombinant proteins as reported earlier [14,21–23]. For this purpose, substrate (MDH, 1.0 μM) was incubated in a 50 mM HEPES (pH 8.0) buffer containing various concentrations of total PaPrx, PpPrx or the protein fractions at 43 °C. Thermal aggregation of the substrate was determined by taking absorbance at 650 nm for 15 min using a spectrophotometer (Evolution 300 UV–VIS spectrophotometer).

2.5. LC–MS analysis and database search

For the identification of disulfide bonding, each protein sample was divided into two identical samples. First sample was initially reduced with 10 mM dithiothreitol (DTT) for 30 min and followed by alkylation with 20 mM iodoacetic acid (IAA) in the dark for 30 min at 37 °C. The mixture was diluted to 5-fold with of ammonium bicarbonate (50 mM, pH 8.0) followed by the addition of trypsin (1:50 protease:substrate ratio) and incubated overnight at 37 °C. The other sample was also digested similarly but without any reduction and alkylation.

Peptides from the protein samples were analyzed using one-dimensional liquid chromatography/tandem mass spectrometry (1D LC–MS/MS) and identified by MS/MS using a nano-LC–MS system equipped with a Nano Acquity UPLC system (Waters, Milford, MA, USA) and an LTQFT mass spectrometer (ThermoFinnigan, Wal-

tham, MA, USA) having a nano-electrospray source. An aliquot (4.0 µL) of the peptide samples was loaded onto a C_{18} trap-column (i.d., 300 µm; length, 5 mm; particle size, 5 µm; Waters) using autosampler and subsequently desalted and concentrated on the column at a flow rate of 5 µL/min. Thereafter, the trapped peptides were back-flushed and separated on a 100 mm microcapillary column consisting of C_{18} (Aqua; particle size 3 µm) packed into 75 µm silica tubing with an orifice i.d. of 6 µm.

The mobile phases, A and B were composed of 0 and 100% acetonitrile each containing 0.1% formic acid. The LC gradient was initially started with 5% B for 5 min and gradually ramped up to 15% B for 5 min followed by 50% B for 55 min, 95% B for 5 min and remained at 95% B over a 5 min period and 5% B for another 5 min period. The column was re-equilibrated with 5% B for 15 min before the next run. A 2.2 kV voltage was applied to produce an electrospray. One high-mass resolution (100,000) MS spectrum was acquired for each duty circle of mass analysis using the FT-ICR analyzer, followed by five data-dependent MS/MS scans using the linear ion trap analyzer. Normalized collision energy (35%) was used throughout the collision-induced dissociation (CID) phase for MS/MS analysis. All MS/MS spectral data were manually analyzed for peptide identification. Oxidized methionine and carbamidomethylated Cys (only for reduced and alkylated protein sample) were considered as a modification [24].

2.6. TEM and single particle image processing

Fractionated proteins were diluted 50-fold with 50 mM HEPES at pH 8.0 for negative staining. After the dilution, 5.0 µL of the final mixture was applied to a glow-discharged carbon-coated grid (Harrick Plasma, Ithaca, NY, USA) for 3 min in air and negatively stained using 1% uranyl acetate (Sigma–Aldrich). Whereas, the proteins were diluted 10-fold with 50 mM HEPES at pH 8.0, mixed with an equal volume of glycerol for metal shadowing. The resulting mixture was sprayed onto freshly cleaved mica and thereafter rotary shadowed with platinum at an angle of 6°. The grids were examined in a Philips CM120 electron microscope (FEI, Hillsboro, OR, USA) at 80 kV. Images were recorded by a $2K \times 2K$ F224HD slow scan CCD camera (TVIPS, Gauting, Germany) at a magnification of $65,000\times$ (0.37 nm/pixel). Single particle image processing was performed using SPIDER (Health Research Inc., Rensselaer, NY, USA) and averaged images were generated by alignment and classification of windowed particles from micrographs [25]. The particles used in the processing were as follows: 239 (F-1; WT-PpPrx); 577 and 1043 (F-1 and F-2; C112S-PpPrx); 459 and 942 (F-1 and F-2; C112A-PpPrx); 261 and 706 (F-1 and F-2; WT-PaPrx); and 592 (F-1; A112C-PaPrx).

2.7. Fluorescence measurement

Hydrophobic domain exposure of the Prx proteins was determined by an Infinite M200 (Tecan Group Ltd., Männedorf, Switzerland), for this purpose spectrum of five Prx proteins was obtained after binding of 10 µL of 10 mM 1,1′-bi(4-anilino)naphthalene-5,5′-disulfonic acid (bis-ANS; Invitrogen Corporation, Carlsbad, CA, USA) to 100 µg of respective Prx proteins. The excitation wavelength was set at 380 nm and emission spectra were monitored from 400 to 600 nm [26].

2.8. Circular dichroism (CD) spectroscopy

Recombinant proteins in 10 mM Tris–HCl (pH 7.4) were used for far ultraviolet (UV)-CD spectral analysis with a Jasco J-715 spectropolarimeter (Jasco Co., Great Dunmow, UK) following the procedure as described earlier [27].

3. Results

3.1. Comparison of peroxidase and molecular chaperone functions between PpPrx and PaPrx proteins

Previously, we have reported that 2-Cys Prxs (PpPrx and PaPrx) from the *Pseudomonas* had both peroxidase and molecular chaperone activities. PpPrx possess considerably lower peroxidase activity but exhibited 40–50-fold higher chaperone activity compared to PaPrx [15,17]. PaPrx exhibited approximately 4–5-fold higher peroxidase activity than that of PpPrx [15,17].

To address the relationship between function and structure, we compared the structure of PpPrx and PaPrx by SEC. When the SEC patterns of PpPrx and PaPrx were compared, only two major peaks were detected for each protein. The majority of PpPrx molecules were present in the first fraction (F-1) and slightly in the second fraction (F-2), whereas PaPrx showed the opposite profile, its molecules were largely present in F-2 fraction and minor in F-1 fraction at the same retention time (Fig. 1A). The proteins (largest multimeric complexes) in the F-1 fraction could not pass through 10% native-polyacrylamide gel due to its large molecular size and therefore retained at the top of the separating gel (Fig. S2). In contrast, the F-2 fraction, consisting of proteins with MWs ranging from about 50 to 300 kDa, contained partial multimer complexes (Fig. S2).

F-1 (HMW protein complexes) and F-2 (LMW forms) fractions displayed opposite pattern in peroxidase and chaperone activities. The F-1 fraction exhibited high chaperone activity and low peroxidase activity, whereas the F-2 fraction displayed high peroxidase activity with low chaperone activity (Fig. 1B). These results suggested that oligomerization of the protein into HMW complexes promotes chaperone activity while dissociation of the HMW complexes into LMW species enhances peroxidase activity. Thus, the switching between the dual functionality of Prxs is associated with their ability to form distinct protein structures (Fig. 1).

To explain the reciprocal activity profiles of PpPrx and PaPrx, we compared their sequence- and structure-based alignments. Both Prxs possessed two highly conserved Cys residues in the same corresponding positions, Cys^{51} and Cys^{171}, and almost identical amino acid sequences. However, PpPrx possessed an additional Cys residue, Cys^{112}, located between the two conserved Cys residues, while PaPrx possessed Ala^{112} (Fig. S1). The additional Cys between the active Cys residues is also found in *Encephalitozoon cuniculi* and *Phytophthora infestans*. It is generally believed that Cys residues function as structural regulatory factors by virtue of their inter- and intra-disulfide bonds and also function as redox sensors by the oxidation and reduction of exposed free cysteines [28,29].

3.2. Effect of Cys^{112} on Prx oligomerization and dual functionality

To address this critical function of an additional Cys residue, we performed site-directed mutagenesis, in which Cys^{112} in PpPrx was substituted with Ser (C112S) or Ala (C112A) and substituting Ala^{112} for Cys (A112C) in PaPrx. Wild type (WT)-Prxs and Prx mutants displayed considerably different structural patterns as evident from the result of non-reducing and native PAGE gels of these proteins (Fig. 2A and B). Various oligomeric protein complexes containing both HMW complexes and several LMW forms were observed in WT-PpPrx. The C112S- and C112A-PpPrx mutants primarily generated dimers as well as fewer HMW complexes than WT-PpPrx (Fig. 2A). On the other hand, the majority of LMW protein species in PaPrx underwent oligomerization to HMW complexes by the replacement of Ala^{112} with Cys (A112C; Fig. 2A and B).
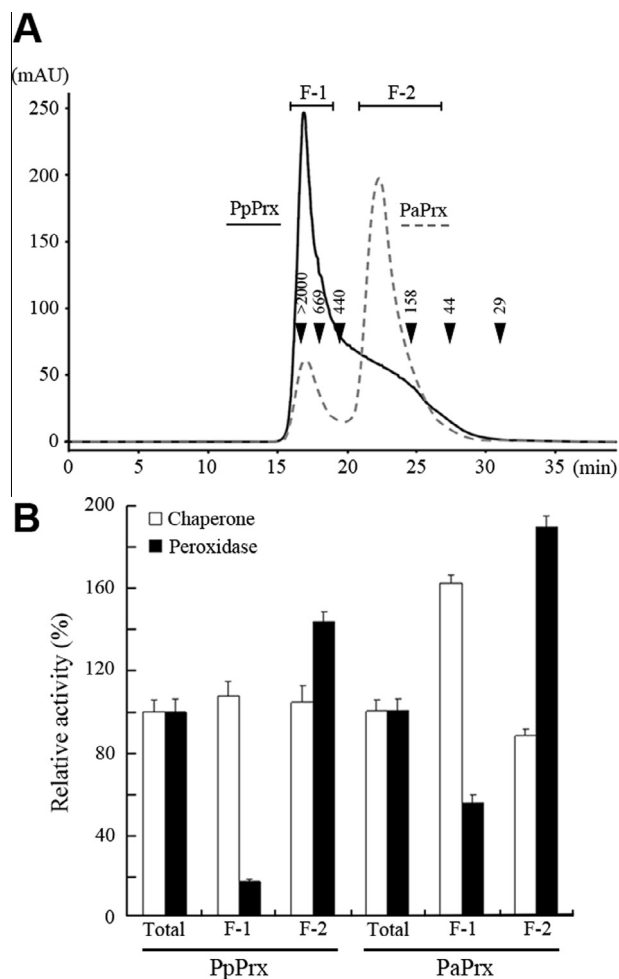
Fig. 1. Structure-dependent regulation of peroxidase and chaperone activities in vitro. (A) SEC analysis of PpPrx and PaPrx proteins. The separated proteins were divided and pooled into two fractions (F-1 and F-2) for further analysis. The numbers in the chromatogram represent the molecular weights of the standard proteins: blue dextran (>2000 kDa), thyroglobulin (669 kDa), ferritin (440 kDa), aldolase (158 kDa), ovalbumin (44 kDa), and carbonic anhydrase (29 kDa). (B) Comparison of structure-dependent enzymatic efficiency (peroxidase and chaperone activities). The two separated fractions (F-1 and F-2) of the PpPrx and PaPrx proteins were compared with each total fraction. The relative activities of the two separated fractions (F-1 and F-2) were compared to those of the respective total fraction, whose activities (peroxidase and chaperone) were set to 100%. The relative activities of the two separated fractions were measured: chaperone (□), peroxidase (■). The data shown are the means of at least three independent experiments.

Fig. 2. Additional Cys-mediated structural and functional changes in two Prxs in vitro. The proteins were separated by 12% non-reducing PAGE (A) or 10% native PAGE (B). (C and D) SEC profiles of WT and Prx mutant proteins. The chromatograms of the Prx mutants were compared to those of each WT-Prx protein. (E) Comparison of changes in additional Cys-mediated enzymatic efficiency (peroxidase and chaperone activities). The Prx mutant proteins were compared with each WT-Prx. The relative activities of Prx mutants were compared to those of the respective predominant activity of each WT-Prx, whose activities (PpPrx: chaperone and PaPrx: peroxidase) were set to 100%. The relative activities of Prx mutants were measured: chaperone (□), peroxidase (■). The data shown are the means of at least three independent experiments.

The SEC profiles of C112S-PpPrx and C112A-PpPrx were compared with those of WT-PpPrx (Fig. 2C). Like native PAGE gel protein patterns, the SEC chromatogram also showed that the protein structures of C112S-PpPrx, C112A-PpPrx, and WT-PaPrx primarily consisted of LMW structures together with a small number of HMW complexes, whereas the predominant forms of WT-PpPrx and A112C-PaPrx were HMW complexes with a small number of LMW species (Fig. 3A–D).

A comparative electron microscopic (EM) analysis demonstrated the prevalence of HMW and LMW complex structures in the F-1 and F-2 fractions, respectively, of the WT and Prx mutants (Fig. 3). The characteristic appearance of HMW complexes in F-1 fractions were resolved by negative staining followed by single particle image processing (Fig. 3A–E). The protein complexes appeared as spherical shapes with a diameter of 20–40 nm (inset averaged images in Fig. 3A–E) suggesting that all WT and mutant proteins are capable of forming spherically shaped oligomers, although the native and non-reducing PAGE results displayed very distinct populations (Fig. 2A and B). In the F-2 fractions of WT-PpPrx and A112C-PaPrx, small featureless particles were visualized in negatively stained and metal-shadowed fields (upper and lower panels in Fig. 3F and J, respectively). Whereas, in the F-2 fractions of WT-PaPrx, C112S-, and C112A-PpPrxs, homogenously distributed particles were visualized in each field (black and white arrowheads in Fig. 3G–I, respectively), adopting a ring-like shape with a consistent diameter of ∼15 nm (Fig. 3K–M, respectively). These results, in conjunction with the SEC results (Fig. 2C and D), suggest that probably Cys[112] in Prxs participates in the instability of LMW oligomeric complexes (Fig. 3F and J), and enhances the for-
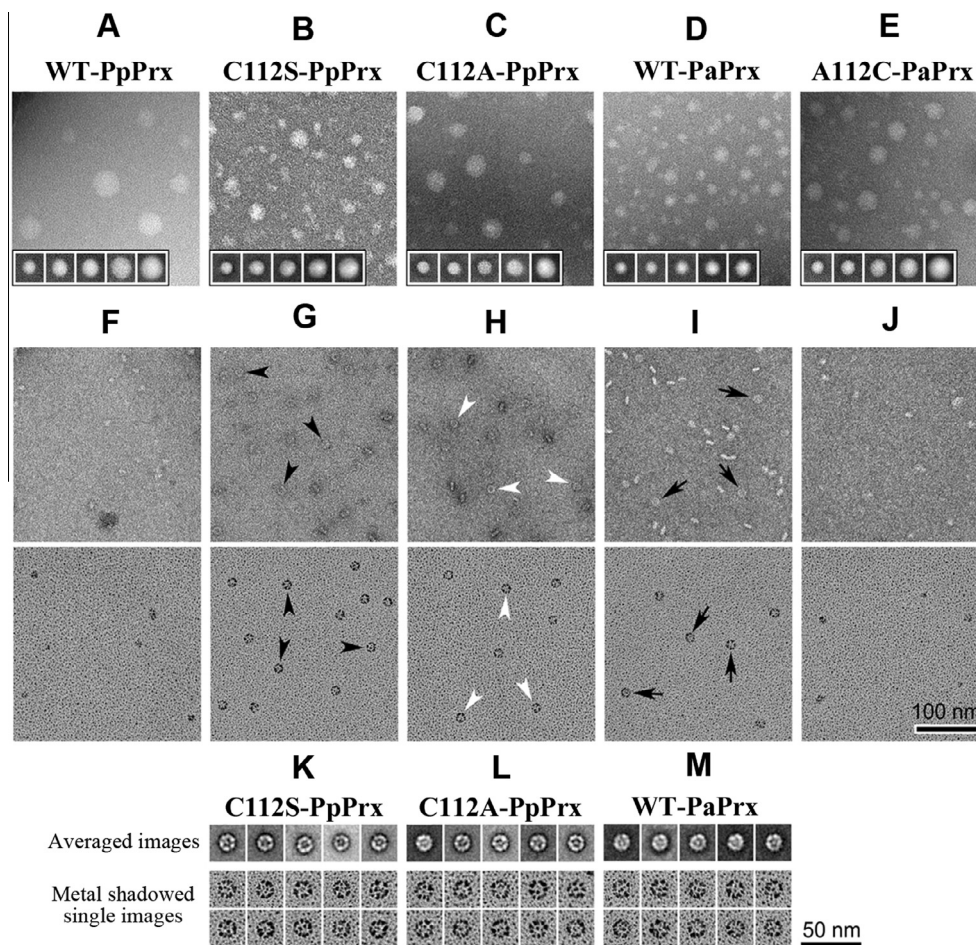
Fig. 3. Observation of additional Cys-mediated structural changes by transmission electron microscopy (EM). (A–E) Negatively stained fields of fractionated proteins taken from high MW fractions (F-1). Insets in each figure display the averaged images of globular-shaped polymers as they appeared in the high MW field. (F–J) Negatively stained images (upper panels in the first row) and metal shadowed images (lower panels in the second row) of middle MW fractions (F-2). Black arrowheads, white arrowheads, and black arrows (G–I) indicate individual ring-shaped complexes found in the fields of C112S-PpPrx, C112A-PpPrx, and WT-PaPrx, respectively. Note that there is no strong evidence for existing ring-shaped oligomers in the fields of WT-PpPrx and A112C-PaPrx (F and J). Scale bar in (J) represents 100 nm in all fields and the inset images (A–J). (K–M) Representative averaged images of ring-shaped oligomers processed from individual complexes from negatively stained fields of (G), (H), and (I) are shown in the top row. Metal shadowed images of individual ring-shaped oligomers are shown in the second and third rows. Averaged images in (A–E) and (K–M) contained 30–70 and 50–90 particles, respectively. Scale bar, 50 nm, applies to the images as shown (K–M).

mation of HMW complexes (Fig. 3A and E). The SEC and EM results confirmed that PpPrx primarily consists of HMW complex structures, whereas PaPrx consists predominantly of oligomeric structures.

To investigate the effect of Cys^{112} in PpPrx and PaPrx on its dual functionality, we compared the peroxidase and molecular chaperone activities of the mutant proteins. The molecular chaperone activity was dramatically decreased in the mutant proteins (C112S or C112A) compared with WT-PpPrx, while the peroxidase activity was significantly increased in these mutants by approximately 4–5-fold higher than WT-PpPrx (Fig. 2E). In contrast, the molecular chaperone activity of WT-PaPrx was increased by approximately 50-fold by the substitution of Cys in place of Ala (A112C), demonstrating that the dual enzymatic activities of A112C-PaPrx were significantly altered to resemble those of WT-PpPrx (Fig. 2E).

After comparing all results of the structural and enzymatic analyses in Figs. 2 and 3, it is concluded that the presence of the additional Cys increases the formation of HMW complex structures with a concomitant increase in chaperone activity. Therefore, we strongly expect that the Cys^{112} residue induces a significant change in protein structure from the LMW structure to HMW complexes by the formation of an inter-disulfide bond (Cys^{112}–Cys^{112}).

3.3. Identification of inter-disulfide linked (Cys^{112}–Cys^{112}) dipeptides by mass spectrometry

In order to explain the increase of HMW complex structures by the Cys^{112} residue of WT-PpPrx and A112C-PaPrx, mass spectrometric analysis of WT-PpPrx and A112C-PaPrx was performed in the presence and absence of dithiothreitol (DTT) treatment to reduce the disulfide bonds. In the LC–MS/MS analysis of tryptic digests without DTT treatment, triply charged monoisotopic molecular ions of inter-disulfide linked (Cys^{112}–Cys^{112}) dipeptides were observed at a mass-to-charge ratio (m/z) of 996.80 for WT-PpPrx and m/z 994.83 for A112C-PaPrx (Fig. 4). Mass differences between experimental and theoretical MW were 7 ppm and 3 ppm, respectively (Table 1). Fig. 4 denotes MS/MS spectra obtained from manually assigned inter-disulfide-linked dipeptides. The dipeptides clearly displayed peptide backbone fragments providing amino acid sequence information, as well as characteristic fragments of disulfide linkage, including Cys persulfide (monomer peptide +32 Da) and dehydroalanine (monomer peptide −34 Da) [24]. During analysis of tryptic digests with DTT and iodoacetamide (IAA) treatments, the carbamidomethylated peptides YTLAADMTHEICcamK for WT-PpPrx and YTLAADTKHEICcamK for A112C-PaPrx were identified rather than inter-disulfide-linked dipeptides (Table 1 and Fig. S3).
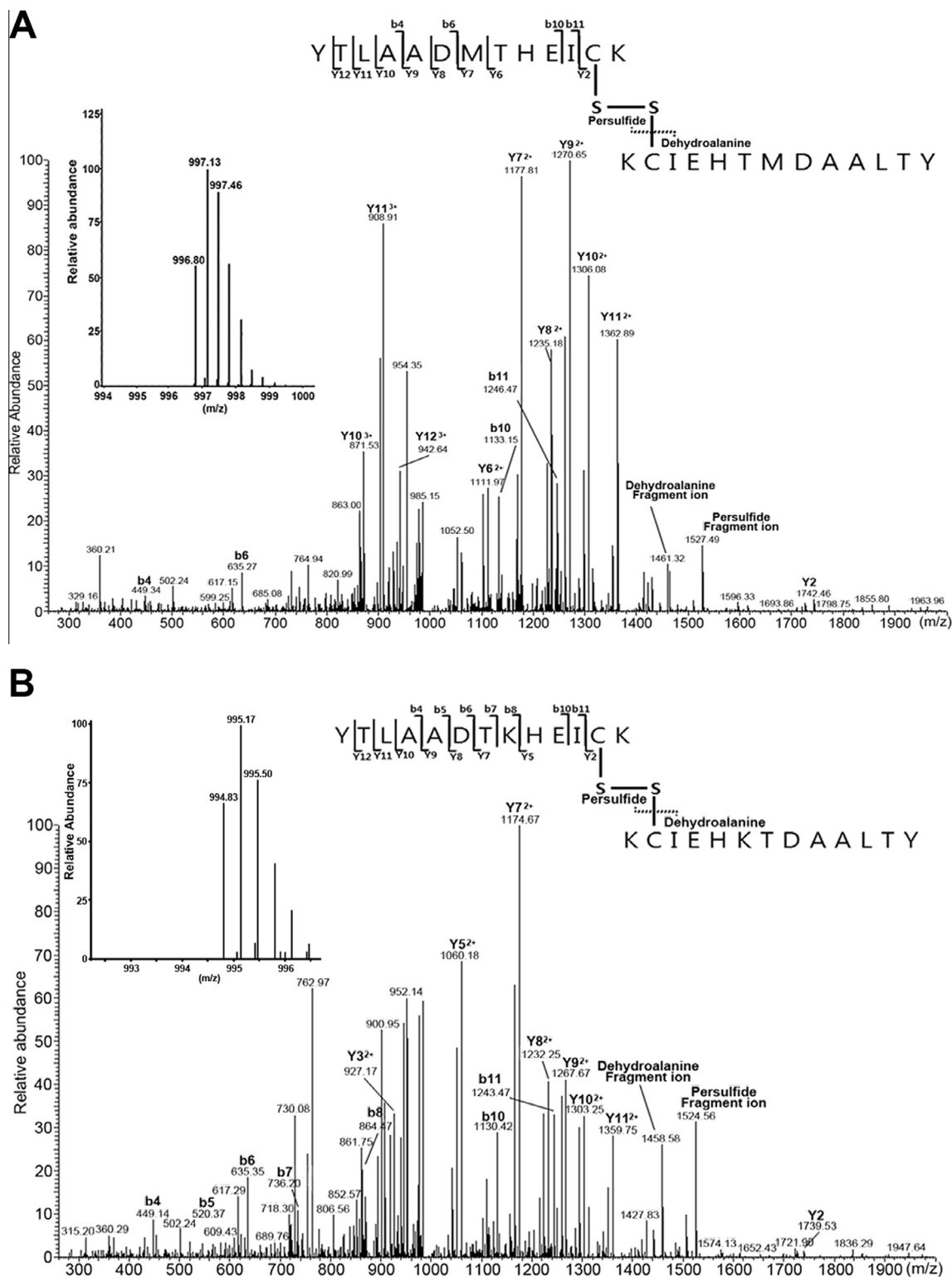
Fig. 4. MS and MS/MS spectra of inter-disulfide linked dipeptides. (A) YTLAADMTHEICK-YTLAADMTHEICK (Cys[112]–Cys[112], theoretical triply charged monoisotopic molecular ion: *m/z* 996.78) from WT-PpPrx. (B) YTLAADTKHEICK-YTLAADTKHEICK (Cys[112]–Cys[112], theoretical triply charged monoisotopic molecular ion: *m/z* 994.82) from A112C-PaPrx. Manual assignment of MS/MS spectra shows fragments of peptide backbone and characteristic fragments of disulfide linkage including cysteine persulfide (monomer peptide +32 Da) and dehydroalanine (monomer peptide −34 Da).

The mass spectrometric results clearly indicate that the Cys[112] residue causes the inter-disulfide bond to link dimer together; therefore, WT-PpPrx and A112C-PaPrx can cause structural alterations from LMW species to HMW complexes by inter-disulfide bond (Cys[112]–Cys[112]; Figs. 2 and 3). Conversely, WT-PaPrx, C112A-PpPrx, and C112S-PpPrx displayed the predomi-

Table 1
Molecular masses of single Cys[112] peptide and inter-disulfide bonded (Cys[112]–Cys[112]) dipeptide depend on DTT.

Protein name	DTT	Peptide sequence	Molecular weight (Da)	Observed ion (m/z)
WT-PpPrx	−	YTLAADMTHEICK KCIEHTMDAALTY S-S	2987.3	996.80 (M+3H)³⁺
WT-PpPrx	+	YTLAADMTHEIC_cam_K	1551.7	776.86 (M+2H)²⁺
A112C-PaPrx	−	YTLAADTKHEICK KCIEHKTDAALTY S-S	2981.5	994.83
A112C-PaPrx	+	YTLAADTKHEIC_cam_K	1548.8	775.39 (M+2H)²⁺

C_cam_: S-carboxyamidomethylcysteine.

Fig. 5. Additional Cys-mediated hydrophobicity and secondary structure changes of the two Prxs in vitro. (A) Fluorescence spectra of bis-ANS bound to 100 μg/mL WT-PpPrx (■), C112A-PpPrx (▲), and C112S-PpPrx (◆). (B) Fluorescence spectra of bis-ANS bound to 100 μg/mL WT-PaPrx (■), and A112C-PaPrx (▲). Both controls (●) were measured in the absence of Prx protein. (C) Changes in the far UV-CD spectra of the five Prx proteins were measured using a protein concentration standard of 100 μg/mL. $[\theta]_M$ is the mean residue mass ellipticity. (D) The comparison of the secondary structure index values was based on the far UV-CD spectra.

nance of LMW structures (Figs. 2 and 3). Thus, the Cys[112] residue is likely to be a regulatory factor for structural and functional changes in PpPrx.

3.4. Effect of Cys[112] on hydrophobicity and secondary structure

The fluorescence levels of bis-ANS bound to C112S-PpPrx and C112A-PpPrx were significantly lower than that of WT-PpPrx (Fig. 5A). However, the fluorescence spectrum of bis-ANS bound

to A112C-PaPrx displayed a significant increase compared to WT-PaPrx (Fig. 5B). These results suggest that the substitution of Cys for Ala (A112C) in WT-PaPrx greatly increased the exposure of hydrophobic domains, resulting in the polymerization of protein into HMW complexes and providing binding sites for partially denatured substrate proteins.

The far-UV CD spectra of the Prxs were used to compare the structural differences between WT Prx and Prx mutant proteins (Fig. 5C and D). The wavelength scan CD spectra in the far ranges

of C112S-PpPrx and C112A-PpPrx demonstrated that the molar ellipticity increased to a greater extent for each mutant spectrum than the WT-PpPrx spectrum due to the substitution of the additional Cys for Ser or Ala (C112S or C112A). In contrast, the spectrum of A112C-PaPrx displayed a greater tendency to decrease molar ellipticity compared to that of WT-PaPrx due to the substitution of Ala with Cys (A112C; Fig. 5C). Changes in secondary structure components stemming from the exclusion of the additional Cys were as follows (Fig. 5D): α-helical content increased from 14.0% to 33.0%, β-sheet content decreased from 40.0% to 21.0%, β-turn content increased from 0% to 17.0%, and random coil content decreased from 46.0% to 28.0%. The substitution of Cys for Ala (A112C-PaPrx) altered the secondary structure components in similar levels to WT-PpPrx as follows: α-helical content decreased from 51.0% to 14.0%, β-sheet content increased from 2.0% to 38.0%, β-turn content decreased from 21.0% to 0.5%, and random coil content increased from 25.0% to 47.0%. Remarkably, these data suggest that the additional Cys functions as a key modulator for both protein function and structure of Prx proteins.

4. Discussion

The present study demonstrates the significance of an additional Cys (Cys^{112}) in the structural and functional switching of 2-Cys Prx of *Pseudomonas* species. PpPrx and PaPrx exhibit dual functions i.e. as peroxidases and/or molecular chaperones, depending on the dynamic and reversible changes in their polymeric structures. In this study, the structural and functional comparisons of PpPrx and PaPrx revealed a novel critical component in the structural polymerization mechanism, namely, that polymerization between subunits can vary in strength and duration. Moreover, the Prx proteins have only a weak tendency to associate with polymerization depending upon environmental conditions, such as, temperature, and pH. Other proteins polymerize dynamically in response to biochemical stimuli, such as, a change in nucleotide binding, hydrophobic interaction, the redox status of Cys residues, or the phosphorylation status of amino acid residues. Such changes can have a dramatic effect on the affinity of the subunits for each other, often by several orders of magnitude [13,30,31].

Homo-oligomeric proteins were originally characterized by their mode of interaction [32]. In general, the factors controlling polymeric assembly of 2-Cys Prxs are poorly understood. Recently an association between local unfolding in the active site with disulfide bond formation and structural rearrangements at the polymerization interface was reported [33]. Such local unfolding process occurs together with the shift of a surface loop driving the structural rearrangements in the interface and leading to decamer dissociation and disulfide bond formation [33]. In contrast, another report proposed that the nucleophilic attack by the resolving Cys (Cys$_R$) on the peroxidatic cysteine sulfenic acid promotes the structural rearrangements at the interface and drives the decamer apart [34]. But the availability of only two forms of the enzyme, the reduced decamer and the disulfide-containing dimer, making it impossible to distinguish between events that occurred immediately prior to dissociation and the structural rearrangements that occurred afterward. König et al. [8] have used five novel variants with specific conformational states e.g. peroxidase function (ΔC), hyperoxidized chaperone (C54D) and oxidized inactive protein (C54DC176K) to demonstrate the importance of structural flexibility for switching between peroxidase and chaperone function. Analysis of CD spectra of reduced and oxidized form these variants revealed that highest percentage of helical arrangement among all variants both under reducing and non-reducing conditions, confirming the expectation that the introduction of negative charge

fosters the compact multimeric state. Apparently a negative charge possibly introduced by phosphorylation strongly affects thiol redox-dependent conformational rearrangements.

Despite having highly conserved sequence- and structure-based alignments, WT-PpPrx and WT-PaPrx, WT-PpPrx consisting primarily HMW complex structure possessed an approximately 40–50-fold stronger molecular chaperone activity than WT-PaPrx, whereas WT-PaPrx existed predominantly in the dimeric LMW form. The chaperone activity was measured based on the thermal aggregation of the substrate, MDH. However, the exact substrates of chaperone proteins in vivo is not known precisely, and interaction of MDH and chaperone has been found stable and well established, therefore MDH was used as a substrate for chaperone activity assay of Prx proteins in the present study. The PpPrx mutants (C112S and C112A) showed similarities with WT-PaPrx in that they displayed a tendency to form polymeric HMW complexes of various MWs, which were converted into LMW structures. This resulted in a significant decrease in molecular chaperone activity and a concomitant increase in peroxidase activity, similar to WT-PaPrx. The substitution of Ala for Cys residue at position 112 in PaPrx caused WT-PaPrx to behave like WT-PpPrx. Further, we identified inter-disulfide (Cys^{112}–Cys^{112})-bonded dipeptides of WT-PpPrx and A112C-PaPrx using mass spectrometry, suggesting that inter-disulfide (Cys^{112}–Cys^{112}) bonding can function by combining dimers into higher-order structures. This function of an additional Cys may clearly explain its effect on structural change of Prx (from LMW to HMW structures). We also investigated the effect of the additional Cys on protein hydrophobicity as related to chaperone function, and the associated change in secondary structure. Our results revealed that various secondary structural elements were transformed by the presence of the additional Cys, thereby providing a structural explanation for the increase in chaperone activity. The additional Cys markedly increased the exposure of the hydrophobic, β-sheet, and random coil-regions, while decreasing the exposure of the α-helix and β-turn regions on the protein structure.

This study provides valuable information related to the functional switch of Prx proteins by explaining the effect of Prx polymeric structures formed due to the presence of the additional Cys on its enzymatic activity. Comparison of the 2-Cys Prx structures, WT-PpPrx and WT-PaPrx, revealed the importance of the additional Cys and led to the identification of the molecular switch responsible for the polymerization. First, we found that the Cys addition and exclusion mutants displayed opposite tendencies in structural and functional switching compared to their wild-type homologs (Figs. 2 and 3), whereby we were able to formulate a comprehensive association model to explain how Prxs are converted into HMW structures that function as molecular chaperones against stress. We were therefore able to explain why WT-PpPrx and WT-PaPrx can have completely different functions as peroxidases or molecular chaperones. Considering the general mechanism for structural changes in other Prxs and WT-PaPrx, perhaps Cys^{112} residue of WT-PpPrx may not be involved in the formation of these dimeric protein structures, because WT-PaPrx and C112S-PpPrx also generated dimeric protein structures under non-reducing conditions (Fig. 2A). The dissociation of HMW complexes into LMW species occurs during the process of removing H$_2$O$_2$, and this structural change activates the peroxidase function of Prx. However, the polymeric structural changes of WT-PpPrx and A112C-PaPrx are caused by the presence of Cys^{112}, which functions as a highly efficient "combiner" of dimers into higher-order structures by inter-disulfide bonding (Cys^{112}–Cys^{112}) between dimer or each dimer (Figs. 2 and 4). The structural change from LMW to HMW complexes is associated with a peroxidase-to-chaperone functional switch.
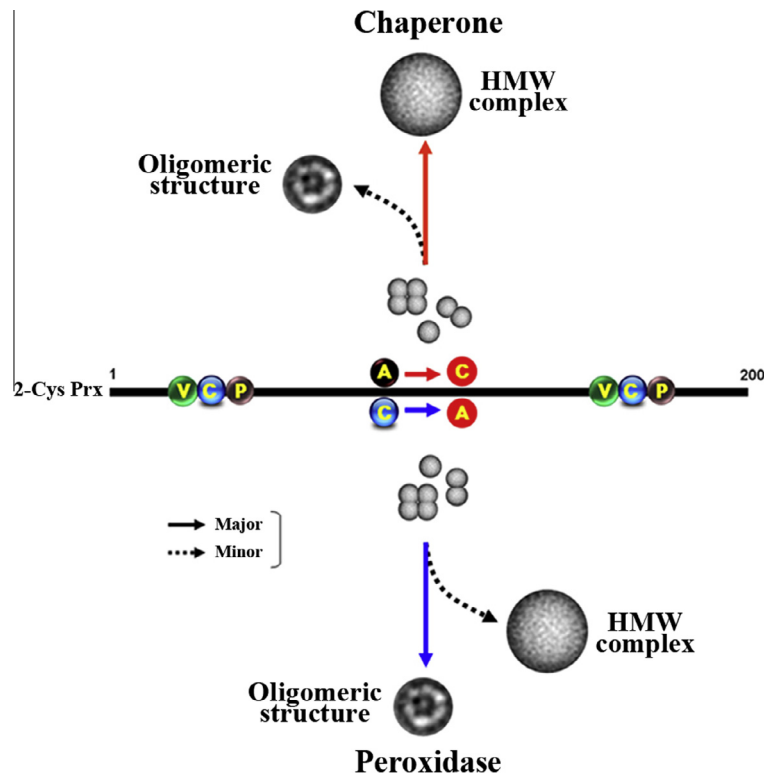
Fig. 6. A model for the additional Cys-dependent structural and functional switching of Prx from peroxidase to a molecular chaperone. In the mechanism involved in regulation of the structural changes, the additional Cys of Prx functions as a highly efficient "polymeric sensor" for HMW complex formation in *Pseudomonas*.

5. Conclusions

The present study demonstrates the participation of Cys[112]-dependent reactions in the oligomerization of 2-Cys Prx protein and regulation of its function during oxidative stress. The model suggested based on the present data may help to explain the reasons for the observation that WT-PpPrx possesses a much greater inhibitory effect on the inactivation of MDH than does WT-PaPrx, even under heat shock conditions. Our experimental evidence with respect to Cys[112] supports the hypothesis that the molecular chaperone function of 2-Cys Prx is increased by the addition of a Cys residue (Fig. 6). The presence of an additional Cys (Cys[112]) in a Prx protein facilitates its polymerization and increases the formation of HMW complex structures as the dominant structures by hydrophobic interactions and inter-disulfide bond formation to link dimer or each dimer together, which act as super-chaperones to prevent the denaturation of protein substrates from external stresses. In contrast, the absence of the additional Cys stabilizes LMW structures of Prx and a reduction in the formation of HMW complex structures. In consequence, LMW structures increase and this structural change induces the peroxidase activity of Prx.

Acknowledgements

Appendix A. Supplementary data

Supplementary data associated with this article can be found, in the online version, at http://dx.doi.org/10.1016/j.febslet.2015.07.046.

References

[1] Bhatt, I. and Tripathi, B.N. (2011) Plant peroxiredoxins: catalytic mechanisms, functional significance and future perspectives. Biotechnol. Adv. 29, 850–859.

[2] Aran, M., Ferrero, D.S., Pagano, E. and Wolosiuk, R.A. (2009) Typical 2-Cys peroxiredoxins-modulation by covalent transformations and noncovalent interactions. FEBS J. 276, 2478–2499.

[3] Tripathi, B.N., Bhatt, I. and Dietz, K.-J. (2009) Peroxiredoxins: a less studied component of hydrogen peroxide detoxification in photosynthetic organisms. Protoplasma 235, 3–15.

[4] Moon, J.C., Kim, G.M., Kim, E.-K., Lee, H.N., Ha, B., Lee, S.Y. and Jang, H.H. (2013) Reversal of 2-Cys peroxiredoxin oligomerization by sulfiredoxin. Biochem. Biophys. Res. Commun. 432, 291–295.

[5] Dietz, K.-J., Jacob, S., Oelze, M.L., Laxa, M., Tognetti, V., de Miranda, S.M., Baier, M. and Finkemeier, I. (2006) The function of peroxiredoxins in plant organelle redox metabolism. J. Exp. Bot. 57, 1697–1709.

[6] Hall, A., Karplus, P.A. and Poole, L.B. (2009) Typical 2-Cys peroxiredoxins-structures, mechanisms and functions. FEBS J. 276, 2469–2477.

[7] Saccoccia, F., Di Micco, P., Boumis, G., Brunori, M., Koutris, I., Miele, A.E., Morea, V., Sriratana, P., Williams, D.L., Bellelli, A. and Angelucci, F. (2012) Moonlighting by different stressors: crystal structure of the chaperone species of a 2-Cys peroxiredoxin. Structure 20, 429–439.

[8] König, J., Galliardt, H., Jütte, P., Schäper, S., Dittmann, L. and Dietz, K.-J. (2013) The conformational bases for the two functionalities of 2-Cysteine peroxiredoxins as peroxidase and chaperone. J. Exp. Bot. 64, 3483–3497.

[9] Dietz, K.-J. (2011) Peroxiredoxins in plants and cyanobacteria. Antioxid. Redox Signal. 15, 1129–1159.

[10] Pulido, P., Spínola, M.C., Kirchsteiger, K., Guinea, M., Pascual, M.B., Sahrawy, M., Sandalio, L.M., Dietz, K.-J., González, M. and Cejudo, F.J. (2010) Functional analysis of the pathways for 2-Cys peroxiredoxin reduction in *Arabidopsis thaliana* chloroplasts. J. Exp. Bot. 61, 4043–4054.

[11] Jang, H.H., Lee, K.O., Chi, Y.H., Jung, B.G., Park, S.K., Park, J.H., Lee, J.R., Lee, S.S., Moon, J.C., Yun, J.W., Choi, Y.O., Kim, W.Y., Kang, J.S., Cheong, G.-W., Yun, D.-J., Rhee, S.G., Cho, M.J. and Lee, S.Y. (2004) Two enzymes in one: two yeast peroxiredoxins display oxidative stress-dependent switching from a peroxidase to a molecular chaperone function. Cell 117, 625–635.

[12] Wen, S.T. and Van Etten, R.A. (1997) The *PAG* gene product, as stress-induced protein with antioxidant properties is an Abl SH3-binding protein and a physiological inhibitor of c-Abl tyrosine kinase activity. Genes Dev. 11, 2456–2467.

[13] Jang, H.H., Chi, Y.H., Park, S.K., Lee, S.S., Lee, J.R., Park, J.H., Moon, J.C., Lee, Y.M., Kim, S.Y., Lee, K.O. and Lee, S.Y. (2006) Structural and functional regulation of eukaryotic 2-Cys peroxiredoxins including the plant ones in cellular defense signaling mechanisms against oxidative stress. Physiol. Plant. 126, 549–559.

[14] Chuang, M.H., Wu, M.S., Lo, W.L., Lin, J.T., Wong, C.H. and Chiou, S.H. (2006) The antioxidant protein alkylhydroperoxide reductase of *Helicobacter pylori* switches from peroxide reductase to a molecular chaperone function. Proc. Natl. Acad. Sci. U.S.A. 103, 2552–2557.

[15] An, B.C., Lee, S.S., Lee, E.M., Lee, J.T., Wi, S.G., Jung, H.S., Park, W. and Chung, B.Y. (2010) A new antioxidant with dual functions as a peroxidase and chaperone in *Pseudomonas aeruginosa*. Mol. Cells 29, 145–151.

[16] Angelucci, F., Saccoccia, F., Ardini, M., Boumis, G., Brunori, M., Di Leandro, L., Ippoliti, R., Miele, A.E., Natoli, G., Scotti, S. and Bellelli, A. (2013) Switching between the alternative structures and functions of a 2-Cys peroxiredoxin, by site-directed mutagenesis. J. Mol. Biol. 425, 4556–4568.

[17] An, B.C., Lee, S.S., Lee, E.M., Lee, J.T., Wi, S.G., Jung, H.S., Park, W., Lee, S.Y. and Chung, B.Y. (2011) Functional switching of a novel prokaryotic 2-Cys peroxiredoxin (PpPrx) under oxidative stress. Cell Stress Chaperons 16, 317–328.

[18] An, B.C., Lee, S.S., Lee, J.T., Hong, S.H., Wi, S.G. and Chung, B.Y. (2011) Engineering of 2-Cys peroxiredoxin for enhanced stress tolerance. Mol. Cells 32, 257–264.

[19] Bradford, M.M. (1976) A rapid and sensitive method for the quantitation of microgram quantities of protein utilizing the principle of protein-dye binding. Anal. Biochem. 72, 248–254.

[20] Chae, H.Z., Robison, K., Poole, L.B., Church, G., Storz, G. and Rhee, S.G. (1994) Cloning and sequencing of thiol-specific antioxidant from mammalian brain: alkyl hydroperoxide reductase and thiol-specific antioxidant define a large family of antioxidant enzymes. Proc. Natl. Acad. Sci. U.S.A. 91, 7017–7021.

[21] Lee, G.J., Roseman, A.M., Saibil, H.R. and Vierling, E. (1997) A small heat shock protein stably binds heat-denatured model substrates and can maintain a substrate in a folding-competent state. EMBO J. 16, 659–671.

[22] Cheong, N.E., Choi, Y.O., Lee, K.O., Kim, W.Y., Jung, B.G., Chi, Y.H., Jeong, J.S., Kim, K., Cho, M.J. and Lee, S.Y. (1999) Molecular cloning, expression, and functional characterization of a 2Cys-peroxiredoxin in Chinese cabbage. Plant Mol. Biol. 40, 825–834.

[23] Moon, J.C., Hah, Y.S., Kim, W.Y., Jung, B.G., Jang, H.H., Lee, J.R., Kim, S.Y., Lee, Y. M., Jeon, M.K., Kim, C.W., Cho, M.J. and Lee, S.Y. (2005) Oxidative stress-dependent structural and functional switching of a human 2-Cys peroxiredoxin isotype II that enhances HeLa cell resistance to H$_2$O$_2$-induced cell death. J. Biol. Chem. 280, 28775–28784.

[24] Choi, S., Jeong, J., Na, S., Lee, H.S., Haynes, P.A., Park, M.K., Fischer, W.H. and Paek, E. (2010) New algorithm for the identification of intact disulfide linkages based on fragmentation characteristics in tandem mass spectra. J. Proteome Res. 9, 626–635.

[25] Burgess, S.A., Walker, M.L., Thirumurugan, K., Trinick, J. and Knight, P.J. (2004) Use of negative stain and single-particle image processing to explore dynamic properties of flexible macromolecules. J. Struct. Biol. 147, 247–258.

[26] Sharma, K.K., Kaur, H., Kumar, G.S. and Kester, K. (1998) Interaction of 1,1′-bi (4-anilino) naphthalene-5,5′-disulfonic acid with alpha-crystallin. J. Biol. Chem. 273, 8965–8970.

[27] Ito, H., Kamei, K., Iwamoto, I., Inaguma, Y., Nohara, D. and Kato, K. (2001) Phosphorylation-induced change of the oligomerization state of alpha B-crystallin. J. Biol. Chem. 276, 5346–5352.

[28] Cumming, R.C., Andon, N.L., Haynes, P.A., Park, M.K., Fischer, W.H. and Schubert, D. (2004) Protein disulfide bond formation in the cytoplasm during oxidative stress. J. Biol. Chem. 279, 21749–21758.

[29] Park, H.J., Choi, Y.D., Song, S.I., Kwon, H.-B., Oh, N.I. and Cheong, J.-J. (2013) Overexpression of the 3′(2′),5′-bisphosphate nucleotidase gene *AtAHL* confers enhanced resistance to *Pectobacterium carotovorum* in *Arabidopsis*. J. Korean Soc. Appl. Biol. Chem. 56, 21–26.

[30] Nooren, I.M.A. and Thornton, J.M. (2003) Structural characterisation and functional significance of transient protein–protein interactions. J. Mol. Biol. 325, 991–1018.

[31] Nooren, I.M.A. and Thornton, J.M. (2003) Diversity of protein–protein interactions. EMBO J. 22, 3486–3492.

[32] Monod, J., Wyman, J. and Changeux, J.-P. (1965) On the nature of allosteric transitions: a plausible model. J. Mol. Biol. 12, 88–118.

[33] Schröder, E., Littlechild, J.A., Lebedev, A.A., Errington, N., Vagain, A.A. and Isupov, M.N. (2000) Crystal structure of decameric 2-Cys peroxiredoxin from human erythrocytes at 1.7 Å resolution. Structure 8, 605–615.

[34] Alphey, M.S., Bond, C.S., Tetaud, E., Fairlamb, A.H. and Hunter, W.N. (2000) The structure of reduced tryparedoxin peroxidase reveals a decamer and insight into reactivity of 2 Cys-peroxiredoxins. J. Mol. Biol. 300, 903–916.